

# Characterization of a synthetic bioactive polymer by nonlinear optical microscopy

N. Djaker,<sup>1,\*</sup> S. Brustlein,<sup>2</sup> G. Rohman,<sup>3</sup> S. Huot,<sup>3</sup> M. Lamy de la Chapelle,<sup>1</sup> and V. Migonney<sup>3</sup>

<sup>1</sup>Université Paris 13, Sorbonne Paris Cité, Laboratoire CSPBAT, CNRS (UMR 7244), 74 rue Marcel Cachin, 93017, Bobigny, France

<sup>2</sup>Institut Fresnel, MOSAIC, CNRS, Aix-Marseille Université, Ecole Centrale Marseille, Domaine Universitaire St Jérôme, France

<sup>3</sup>Université Paris 13, Sorbonne Paris Cité, Laboratoire CSPBAT, CNRS (UMR 7244), 99 avenue JB Clément, 93430, Villetaneuse, France

\*[nadia.djaker@univ-paris13.fr](mailto:nadia.djaker@univ-paris13.fr)

**Abstract:** Tissue Engineering is a new emerging field that offers many possibilities to produce three-dimensional and functional tissues like ligaments or scaffolds. The biocompatibility of these materials is crucial in tissue engineering, since they should be integrated in situ and should induce a good cell adhesion and proliferation. One of the most promising materials used for tissue engineering are polyesters such as Poly- $\epsilon$ -caprolactone (PCL), which is used in this work. In our case, the bio-integration is reached by grafting a bioactive polymer (pNaSS) on a PCL surface. Using nonlinear microscopy, PCL structure is visualized by SHG and proteins and cells by two-photon excitation autofluorescence generation. A comparative study between grafted and nongrafted polymer films is provided. We demonstrate that the polymer grafting improves the protein adsorption by a factor of 75% and increase the cell spreading onto the polymer surface. Since the spreading is directly related to cell adhesion and proliferation, we demonstrate that the pNaSS grafting promotes PCL biocompatibility.

© 2013 Optical Society of America

**OCIS codes:** (160.1435) Biomaterials; (180.4315) Nonlinear microscopy.

## References and links

1. D. W. Hutmacher, J. T. Schantz, C. X. F. Lam, K. C. Tan, and T. C. Lim, "State of the art and future directions of scaffold-based bone engineering from a biomaterials perspective," *J. Tissue. Eng. Regen. M.* **1**(4), 245–260 (2007).
2. M. Ciobanu, A. Siove, V. Gueguen, L. Gamble, D. Castner, and V. Migonney, "Radical graft polymerization of styrene sulfonate on poly(ethylene terephthalate) films for ACL applications: Grafting from and chemical characterization," *Biomacromolecules* **7**(3), 755–760 (2006).
3. G. Helary, F. Noirclere, J. Mayingi, and V. Migonney, "A new approach to graft bioactive polymer on titanium implants: Improvement of MG 63 cell differentiation onto this coating," *Acta Biomater.* **5**(1), 124–133 (2009).
4. G. Pavon-Djavid, L. J. Gamble, M. Ciobanu, V. Gueguen, D. G. Castner, and V. Migonney, "Bioactive poly(ethylene terephthalate) fibers and fabrics: Grafting, chemical characterization, and biological assessment," *Biomacromolecules* **8**(11), 3317–3325 (2007).
5. Z. Cheng and S. Teoh, "Surface modification of ultra thin poly (epsilon-caprolactone) films using acrylic acid and collagen," *Biomaterials* **25**(11), 1991–2001 (2004).
6. L. Savarino, N. Baldini, M. Greco, O. Capitani, S. Pinna, S. Valentini, B. Lombardo, M. T. Esposito, L. Pastore, L. Ambrosio, S. Battista, F. Causa, S. Zeppetelli, V. Guarino, and P. A. Netti, "The performance of poly-epsilon-caprolactone scaffolds in a rabbit femur model with and without autologous stromal cells and BMP4," *Biomaterials* **28**(20), 3101–3109 (2007).

7. M. A. Woodruff, and D. W. Huttmacher, "The return of a forgotten polymer: Polycaprolactone in the 21st century," *Prog. Polym. Sci.* **35**(10), 1217–1256 (2010)
8. T. Desmet, R. Morent, N. De Geyter, C. Leys, E. Schacht, and P. Dubruel, "Nonthermal Plasma Technology as a Versatile Strategy for Polymeric Biomaterials Surface Modification: A Review," *Biomacromolecules* **10**(9), 2351–2378 (2009).
9. F. El Khadali, G. Helary, G. Pavon-Djavid, and V. Migonney, "Modulating fibroblast cell proliferation with functionalized poly(methyl methacrylate) based copolymers: Chemical composition and monomer distribution effect," *Biomacromolecules* **3**(1), 51–56 (2002).
10. D. Le Guillou-Buffello, G. Helary, M. Gindre, G. Pavon-Djavid, P. Laugier, and V. Migonney, "Monitoring cell adhesion processes on bioactive polymers with the quartz crystal resonator technique," *Biomaterials* **26**(19), 4197–4205 (2005).
11. J. Zhou, M. Manassero, V. Migonney, and V. Viateau, "Clinic and biological evaluation of synthetic bioactive ligament prosthesis in sheep," *Irbm* **30**(4), 153–155 (2009).
12. I. W. Hamley, V. Castelletto, R. V. Castillo, A. J. Muller, C. M. Martin, E. Pollet, and P. Dubois, "Crystallization in poly(L-lactide)-b-poly(epsilon-caprolactone) double crystalline diblock copolymers: A study using X-ray scattering, differential scanning calorimetry, and polarized optical microscopy," *Macromolecules* **38**(2), 463–472 (2005).
13. J. Xu, J. Bao, B. Guo, H. Ma, T. L. Yun, L. Gao, G. Q. Chen and T. Iwata, "Imaging of nonlinear optical response in biopolyesters via second harmonic generation microscopy and its dependence on the crystalline structures," *Polymer* **48**, 348–355 (2007).
14. W. Zipfel, R. Williams, and W. Webb, "Nonlinear magic: multiphoton microscopy in the biosciences," *Nat. Biotechnol.* **21**(11), 1368–1376 (2003).
15. P. Campagnola, A. Millard, M. Terasaki, P. Hoppe, C. Malone, and W. Mohler, "Three-dimensional high-resolution second-harmonic generation imaging of endogenous structural proteins in biological tissues," *Biophys. J.* **282**, 493–508 (2002).
16. K. Konig, K. Schenke-Layland, I. Riemann, and U. Stock, "Multiphoton autofluorescence imaging of intratissue elastic fibers," *Biomaterials* **72**(26), 495–500 (2005).
17. S. Bancelin, C. Aime, T. Coradin, and M. C. Schanne-Klein, "In situ three-dimensional monitoring of collagen fibrillogenesis using SHG microscopy," *Biomed. Opt. Express* **3**(6), 1446–1454 (2012).
18. P. J. Campagnola and L. M. Loew, "Second-harmonic imaging microscopy for visualizing biomolecular arrays in cells, tissues and organisms," *Nature Biotechnology* **21**(11), 1356–1360 (2003).
19. A. Zoumi, A. Yeh, and B. J. Tromberg, "Imaging cells and extracellular matrix in vivo by using second-harmonic generation and two-photon excited fluorescence," *PNAS* **99**(17), 11014–11019 (2002).
20. E. Filova, Z. Burdikova, M. Rampichova, P. Bianchini, M. Capek, E. Kostakova, E. Amler, and L. Kubinova, "Analysis and three-dimensional visualization of collagen in artificial scaffolds using nonlinear microscopy techniques," *J. Biomed. Optics* **15**(6), (2010).
21. W. Y. Hu, G. Zhao, C. Y. Wang, J. G. Zhang, and L. Fu, "Nonlinear Optical Microscopy for Histology of Fresh Normal and Cancerous Pancreatic Tissues," *Plos One* **7**(5), (2012).
22. K. Konig, P. T. C. So, W. W. Mantulin, B. J. Tromberg, and E. Gratton, "Two-photon excited lifetime imaging of autofluorescence in cells during UVA and NIR photostress," *J. MICROSC-OXFORD* **183**(3), 197–204 (1996).
23. X. F. Wu, G. Chen, J. P. Lu, W. F. Zhu, J. T. Qiu, J. X. Chen, S. S. Xie, S. M. Zhuo, and J. Yan, "Label-Free Detection of Breast Masses Using Multiphoton Microscopy," *Plos One* **8**(6), (2013).
24. M. Cai, M. Stankova, S. J. K. Pond, A. V. Mayorov, J. W. Perry, H. I. Yamamura, D. Trivedi, and V. J. Hruby, "Real Time Differentiation of G-Protein Coupled Receptor (GPCR) Agonist and Antagonist by Two Photon Fluorescence Laser Microscopy," *JACS* **126** (23), 7160–7161 (2004).
25. K. Wang, T. M. Liu, J. Wu, N. G. Horton, C. P. Lin, and C. Xu, "Three-color femtosecond source for simultaneous excitation of three fluorescent proteins in two-photon fluorescence microscopy," *Biomed. Opt. Express* **3**(9), 1972–1977 (2012).
26. G. Helary, F. Noirclere, J. Mayingi, B. Bacroix, and V. Migonney, "A bioactive polymer grafted on titanium oxide layer obtained by electrochemical oxidation. Improvement of cell response," *J. MATER. SCI-MATER. M.* **21**(2), 655–663 (2010).
27. A. Michiardi, G. Helary, P. C. T. Nguyen, L. J. Gamble, F. Anagnostou, D. G. Castner, and V. Migonney, "Bioactive polymer grafting onto titanium alloy surfaces," *Acta Biomater.* **6**(2), 667–675 (2010).
28. S. Brustlein, P. Ferrand, N. Walther, S. Brasselet, C. Billaudeau, D. Marguet, and H. Rigneault, "Optical parametric oscillator-based light source for coherent Raman scattering microscopy: practical overview," *J. Biomed. Opt.* **16**(2), (2011).
29. D. W. Grainger, G. Pavon-Djavid, V. Migonney, and M. Josefowicz, "Assessment of fibronectin conformation adsorbed to polytetrafluoroethylene surfaces from serum protein mixtures and correlation to support of cell attachment in culture," *J. BIOMAT. SCI-POLYM. E.* **14**(9), 973–988 (2003).

## 1. Introduction

Polyesters are widely used in tissue engineering because of their flexibility, elasticity and mechanical strength and resistance at break and friction [1]. Unfortunately, most of these polyesters suffer from their low surface energy leading to a hydrophobic surface which decreases their biocompatibility. To overcome this drawback, a surface modification of these polyesters is often needed to make them hydrophilic which improves their biocompatibility, promoting cell adhesion, growth and proliferation and to make them suitable for implants or scaffolds [2–4].

Poly( $\epsilon$ -caprolactone) (PCL) is a biodegradable polyester soluble in solvents organic which have been widely proposed for tissue engineering applications [5–7]. One of the main solutions to make PCL more biocompatible is to modify its surface by grafting another polymer more suitable for biological media [8]. Usually, a synthetic polymer such as poly(sodium styrene sulfonate) (pNaSS) is grafted onto the surface of the polyesters [2, 3].

The grafting of such anionic polymer onto implant surfaces leads to interesting biological properties such as modulation of protein conformation, cell adhesion and proliferation which improve the biocompatibility of the grafted implants or scaffolds [9, 10]. In biocompatible prosthesis, the surface promotes the formation of a layer of controlled adsorbed proteins (the nature, amount and conformation) that stimulates adhesion, spreading and proliferation of fibroblasts and cause a minimal inflammatory response during long-term remodeling [11].

PCL is an aliphatic polyester with a semi-crystalline structure at room temperature. The crystalline lamellae and amorphous phase are organized into semi-crystalline arrangements whose size can vary from micrometers to several millimeters. The most commonly encountered microstructures are spherulites, which are characterized by a radial arrangement of crystalline lamellae from the core and are separated from one to another by the amorphous phase. The optical properties of the spherulites, such as their sensitivity to light polarization, result from the dielectric nature of the polymer and its highly anisotropic semi-crystalline structure [12]. Some of these polyesters offers another optical property as second harmonic generation (SHG) depending on their composition and structure [13]. The optical imaging of spherulites structure is then possible by using SHG microscopy.

Generally, SHG microscopy is a nonlinear optical process which is already widely used in biological imaging [14]. It allows inherent deep tissue penetration [15, 16], high 3D spatial resolution and preserves the samples from modifications induced by staining procedures. Since SHG is based on a second order nonlinear optical process, it is sensitive to the molecular structures, enabling a strong imaging contrast for non-centrosymmetric molecular ordered structures such as collagen fibers in tissues or polymers [13, 17]. SHG and two-photon excitation fluorescence (TPEF) microscopy are often combined for optical imaging [18, 19]. TPEF is a nonlinear optical process which is widely used in scaffolds imaging [20], label-free cells imaging [21–23] and proteins characterization [24, 25].

The aim of this study is to characterize PCL films before and after surface modification by grafting pNaSS polymer. This characterization is reached by initially comparing proteins adsorption in both surfaces by measuring proteins two-photon excitation autofluorescence signal and PCL films SHG signal. It is essential to understand if proteins adhere differently to grafted PCL and unmodified films and if that difference is significantly related to cell morphology which a very important parameter for cell adhesion and proliferation [26, 27].

Since spreading plays an important role in the adhesion and cell proliferation, PCL films were incubated with fibroblast cells in order to compare cell surface area in both cases (grafted and non grafted films). The study of cell morphology by TPEF microscopy was performed on non-labeled cytoplasm and statistical calculations of the surface cell area provided quantitative measurements on cell spreading difference between grafted and unmodified films.

## 2. Experimental

### 2.1. Polymer films preparation, grafting of pNaSS and sterilization

Polymer films were made from Poly( $\epsilon$ -caprolactone) (PCL,  $M_w = 40,000 \text{ g}\cdot\text{mol}^{-1}$ , PDI = 1.6) (Sigma Aldrich). PCL solution in dichloromethane (60 (w/v)%) was dropped off on a glass slide and spin-coated for 30 seconds at 1500 rpm. The films were air-dried for 2 hours and then vacuum-dried for 24 hours to remove the solvent, and finally cut into disks of 1.6 cm diameter with a  $50 \mu\text{m}$  thickness. The PCL film surface was modified through the grafting of pNaSS using a "grafting from" technique developed by the authors [2] and adapted to PCL to avoid polymer degradation. The pNaSS grafting is carried out as following: films were suspended into distilled water and ozone was generated using an ozone generator (BMT 802N-ACW) with a pressure of 0.5 bar and an oxygen flow rate of  $0.6 \text{ L}\cdot\text{min}^{-1}$ . The reaction time was 20 minutes at room temperature and under stirring.

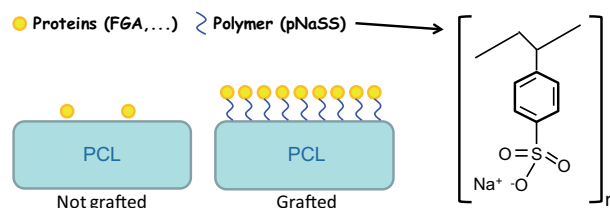


Fig. 1. Schematic presentation of nongrafted and grafted PCL films.

Concomitantly, a NaSS solution in distilled water (15 (w/v)%), containing Mohr's salt (2.5 w% -Sigma Aldrich), had been degassed and warmed at  $45^\circ\text{C}$ . After ozonation, PCL films were transferred in the NaSS solution and the system was maintained at  $45^\circ\text{C}$  for 3 hours. After polymerization, the samples were washed with distilled water overnight and finally vacuum-dried. Films were sterilized by immersing them in 70 v.% ethanol for 2 hours, then in sterile PBS solution for 2 hours.

The quantitative amount of pNaSS grafted onto PCL film was determined through a colorimetric method based on complexation of BT (toluidine blue) with the sulfonate groups [27]. The grafting density of pNaSS was found to be  $5 \cdot 10^{-8} \text{ mol cm}^{-2}$ . This method has also allowed to put in evidence that the pNaSS grafting was homogeneous all over the film surface and that the complexation of BT was only due to the presence of pNaSS, as the control with a non-grafted film remains colorless.

### 2.2. Nonlinear microscopy

The multimodal nonlinear microscope used in these experiments was described previously in [28]. The excitation is provided by an OPO (optical parametric oscillators), which is a picosecond mode-locked frequency ( $5 \text{ ps} / 76 \text{ Mhz}$ ) pumped by a Nd:YVO-laser (HighQ laser-Austria) operating at 532 nm and delivering 4W of green output power. The oscillator emits 780 nm wavelength with 10 mW power and the excitation is sent onto a couple of galvanometric scanning mirrors (Cambridge Technology). The backward emitted light (SHG and TPEF) is collected by the focusing objective (x40, 1.15NA, Olympus) lens and focused on two photomultipliers (CPM-C972, Perkin Elmer Optoelectronics) that detect separately via emission filters: SHG at 390 nm (15 nm bandwidth, Chroma Technology) and TPEF at  $525 \pm 75 \text{ nm}$  (Chroma Technology). The dual-axis driver (Cambridge Technology- scanning area  $200 \times 200 \mu\text{m}^2$ ) and the photon counting signal from the PMT are recorded using dedicated input/output electronic boards (National Instruments).

Combined SHG/TPEF signals were recorded for each sample to make two-dimensional images at 5  $\mu\text{m}$  of depth inside the sample (optical cross-section, acquisition time of 10 s/image). To avoid cells photodamage excitation was reduced to 1mW. Three-dimensional images were made by combining 20 records of SHG/TPEF images in 20  $\mu\text{m}$  depth to visualize the whole spherulite surface (one 2D image recorded for each 1  $\mu\text{m}$  depth, 3D image construction time about 20 min). Image processing was performed by Igor software (Igor Pro, WaveMetrics USA).

### 2.3. PCL films incubation with proteins or cells

Sterilized PCL films were placed in individual wells of a 24-well plate. After that, the substrates were soaked independently in four different media and incubated at 37°C :

Medium 1 (without proteins): PBS - Phosphate buffered saline.

Medium 2 (10 % protein mixture): CM- Culture medium: Dulbecco's modified eagle medium, 1% L-glutamine, 1% penicillin-streptomycin , 10% foetal bovine serum were supplied by Gibco (USA).

Medium 3 (10 % a single protein): FGA- 10% of Fibrinogen glycoprotein (FGA) stabilized with 1% of albumin.

Medium 4 (Cells)- McCoy fibroblast cells in a culture medium.

The proteins/films incubation time was about 2 hours (after 2 hours, the film surface incubated with 10% of proteins concentration -medium 2 and 3- is saturated). Whereas, the cells/films incubation time was about 48 hours (the cells are in the latency phase -before division- and this time is necessary to see the cell spreading -medium 4-). PCL films were rinsed three times with sterile PBS (buffer solution) before observation and imaging. For each experiment, two films were incubated in each medium, in same conditions and six images were taken for each sample. Statistics were calculated on integrated TPEF signal in 7 spherulites (n=7) for each condition. Data were expressed as mean value  $\pm$  s.d. unless indicated otherwise and analyzed using one-way analysis of variance (ANOVA). The degree of significance is indicated when appropriate (\*p < 0.05 "significant"; \*\*p < 0.01 "more significant"; \*\*\*p < 0.001 "very significant").

### 2.4. Cell culture

Human McCoy fibroblast cell line was purchased from the American Type Cultures Collection (ATCC - CRL-1696, USA) and stored frozen. Sterilized PCL films were placed in individual wells of a 24-well plate and weighed down with teflon inserts. McCoy cells were seeded onto the films at a cell density of 50,000 cells/well for 2 hours at 37 °C. Wells were flooded with complete medium above the teflon ring and incubated at 37 °C in a humidified atmosphere of 5 % CO<sub>2</sub> in air.

## 3. Results and discussion

Grafted and non grafted PCL films are characterized by nonlinear microscopy. The film surface grafting with pNaSS polymer makes the films hydrophilic, increases protein adsorption (see Fig. 1) which induce more cell adhesion and promote films biocompatibility. While PCL polymer produce SHG signal, pNaSS polymer, proteins and cells are visualized by two-photon excitation autofluorescence microscopy. Both grafted (Fig. 2 up) and non grafted (Fig. 2 down) PCL film optical cross-sections are recorded by measuring simultaneously SHG (in green) and TPEF (in red) signals at the same depth (5  $\mu\text{m}$ ).

The SHG efficiency depends on both the chemical and crystalline structure of the polymer. It was observed that SHG in polyesters is due to the carbonyl groups and it was reported that for an identical conformation of the polymeric chains, the orientation of these groups exhibits



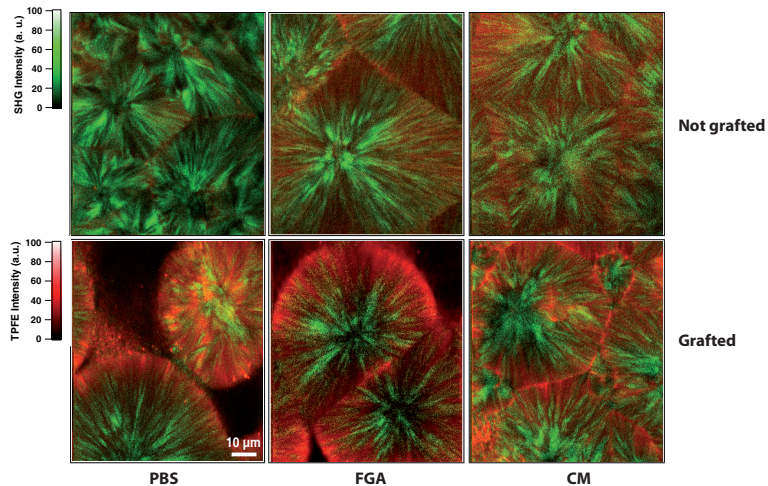


Fig. 2. TPEF (in red) and SHG (in green) images of nongrafted (up) and grafted PCL films (down) after incubation in different media 1, 2 and 3. The images are  $300 \times 300$  pixel and the pixel dwell time is  $50 \mu\text{s}$ . Excitation power at  $10\text{mW}$ .

different SHG efficiency due to different packing schemes of the chain stems in the crystal lattice [13]. Thus in Fig. 2, the SHG signal (in green color) clearly exhibits the spherulitic structure of the PCL films. The SHG is emitted by the crystalline phase in green (no SHG for amorphous phase). In the case of films incubated with only PBS (medium 1 without proteins), the grafted PCL shows a TPEF signal (in red) only due to the pNaSS polymer. The red coloration demonstrates the presence of pNaSS onto the film and confirms the quite homogeneous grafting as found with the colorimetric method with toulidine blue. The SHG images of PCL films show the presence of some voids between spherulites on the film surface due to the spin-coating method. These voids appear in black.

Both pNaSS grafted and nongrafted PCL films were incubated with the different media containing one (FGA -medium 3-) or several (medium 2) proteins to observe the specificity of the grafting on the protein-surface adsorption. In the case of films incubated with only PBS (medium 1 without proteins), the grafted PCL shows a TPEF signal only due to the pNaSS polymer. For both media 2 and 3, where proteins (FGA and CM) are present, the fluorescence signal increases for the grafted films compared to the one obtained for nongrafted films. Thus, the number of proteins adsorbed on the surface is higher for the grafted films compared to the nongrafted one. It demonstrates clearly that only few proteins naturally adsorb at the surface of the nongrafted films whereas the grafting increases the proteins adsorption. This observation is more visible by the three-dimensional TPEF/SHG images in Fig. 3. Indeed, a few red dots appear on the non-grafted PCL surface confirming the very little protein adsorption. On the contrary, the pNaSS and FGA protein signal covers homogeneously the whole grafted film surface which confirms the homogeneity of both pNaSS grafting and protein adsorption on pNaSS. Moreover, the thickness attributed of the TPEF signal is quite large because the pNaSS is in a swollen state in aqueous medium and the pNaSS polymeric chains are unfolded. This pNaSS swollen state also allows a better protein adsorption as the specific surface accessible to protein increases.

In order to characterize this specificity, TPEF signals were quantified from the recorded 2D-images in all cases: without proteins (medium 1), several proteins which constitute the cell culture medium (medium 2) and finally, a specific protein (FGA) which have a good affinity

with grafted surface films (medium 3).

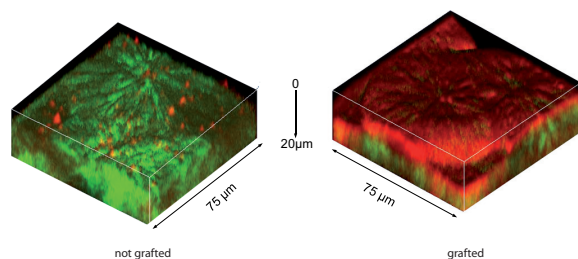


Fig. 3. Three-dimensional TPEF (red) and SHG (green) images of grafted (right) and non-grafted (left) PCL films incubated with FGA proteins (medium 3). Excitation power at 10mW.

The fluorescence signal is linearly dependent on the proteins number, this gives access to a quantitative description of proteins adsorption on PCL films. TPEF signal integration was plotted in Fig. 4. TPEF signal was measured in one spherulite surface ( $60 \times 60 \mu m^2$ ) for both grafted and nongrafted films in media 1, 2 and 3. By taking 7 two-dimensional spherulite images in each case, we obtain an average TPEF signal and a standard deviation around 3% (see Fig. 4). For nongrafted films, TPEF signal is about  $0.6 \cdot 10^6$  counts for medium 1, this value represents the background signal since medium 1 doesn't contain any protein or pNaSS,  $1.2 \cdot 10^6$  counts for medium 2 and  $1.3 \cdot 10^6$  counts for medium 3 (TPEF signal of adsorbed proteins in both cases). For grafted films, the TPEF signal is about  $10.9 \cdot 10^6$  counts for medium 1 (pNaSS TPEF signal) and around  $2.2 \cdot 10^6$  counts for medium 2 and  $2.3 \cdot 10^6$  counts for medium 3 (contribution of both pNaSS and proteins).

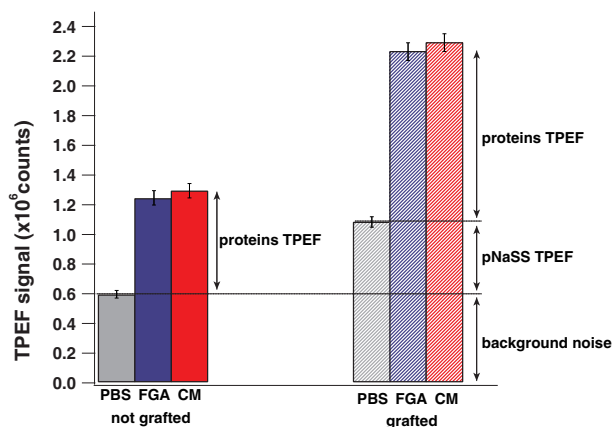


Fig. 4. Integrated TPEF signal in one spherulite for both grafted and nongrafted films in media 1, 2 and 3.

By removing the background signal, we can estimate that the fluorescence signal of pNaSS represents 30%, while the proteins signal is about 70% of the total emitted TPEF signal (pNaSS and proteins). The difference of protein adsorption between medium 2 and 3 is not noticeable, which is in agreement with the fact that each medium contains the same amount of proteins (10 %). In the case of nongrafted films, the TPEF signal resulting from the adsorbed proteins, represents only 40% of the TPEF signal recorded in the case of the grafted films. We conclude

that the grafting increases by 75% the proteins adsorption which is in a good agreement with the authors previous results [26, 27].

The cell morphology and adhesion play a critical role in the formation of tissues and organs and is generally a main indicator of the viability of most of the cells. Thus, such observation gives important information on the biocompatibility of the polymer films. In Fig. 5, McCoy fibroblast cells on PCL films were shown by TPEF microscopy. Cell cytoplasm was observed in red color, whereas the nucleus appears as a darker central region. In the case of grafted films, the film surface is totally covered by cells, which look better spread in comparison with the non-grafted film. Cell surface area for both grafted and nongrafted films was calculated taking 7 cells in the TPEF images in each case. Data were expressed as mean value  $\pm$  s.d. and a high statistical degree of significance was obtained comparing cells surface area for both grafted and non grafted films (\*\* $p < 0.001$ ).

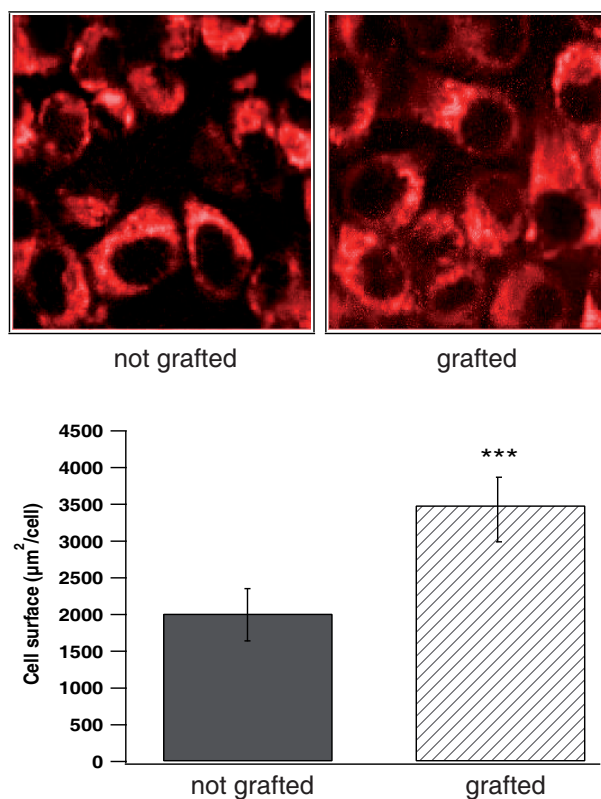


Fig. 5. TPEF (red) and SHG (green) images of grafted (right) and nongrafted (left) PCL films incubated with McCoy fibroblast cells. Each image is ( $75 \mu\text{m} \times 75 \mu\text{m}$ ) size. Excitation power at 1mW. (Down) Calculated cell surface area for both grafted and nongrafted films. Data are expressed as mean  $\pm$  s.d. ( $n = 7$ ); where \*\*\* $p < 0.001$  (ANOVA).

For grafted films, the cells surface was ( $3490.45 \pm 445$ )  $\mu\text{m}^2/\text{cell}$ , whereas, cells surface was about ( $2014.81 \pm 366$ )  $\mu\text{m}^2/\text{cell}$  in the case of nongrafted films (Fig. 5). This clearly indicates that the cell spreading was better in the case of grafted films, which leads to a better cell adhesion, as previously observed by the authors in other pNaSS grafted titanium [26, 27]. This also suggests that the pNaSS grafting, by increasing the cell spreading, promotes biocompatibility of PCL films.



#### **4. Conclusion**

TPEF and SHG microscopy was an important tool in this study to reveal PCL polymer structure (SHG) and proteins and cells imaging (TPEF). PCL films were grafted by pNaSS polymer to increase their biocompatibility by enhancing protein adsorption on the PCL film surface at 75%. This biocompatibility was also demonstrated by a spreading measurement calculating the cell surface area on PCL films. The cell spreading has more than doubled in the case of grafted PCL. This work takes full advantage of the abilities of nonlinear microscopy to two- and three-dimensional imaging of polymer tissues and cells providing qualitative information (proteins adsorption on films surfaces) and relative protein quantification, enabling unique insights in the protein/polymer and cell/polymer interactions.

#### **Acknowledgments**

This research was partly supported by the Région Provence Alpes Côte dAzur and by the French Agence Nationale de la Recherche under contract no. ANR-10-INBS-04-01 France Bio Imaging. The authors thank useful discussions on fluorescence microscopy with Dr.Herv Rigneault and Dr. Patrick Ferrand (Institut Fresnel Mosaic, Marseille, France).